Viscous free surface cusps - local solution

J. Eggers
School of Mathematics, University of Bristol, Fry Building, Woodland Road, Bristol BS8 1UG, United Kingdom

Free surface cusps appear as a generic feature in viscous flow with a free surface. However, a mathematical description has so far only been possible by constructing exact solutions to the Stokes equation in very specific and idealized geometries, using complex mapping techniques. Here we use the boundary integral formulation of the Stokes equation to show that cusps are local singular solutions to Stokes' equation. We recover Jeong and Moffatt's [J. Fluid Mech. **241**, 1, (1992)] local cusp solution in the limit of vanishing cusp curvature, demonstrating its universality across all viscous flows.

I. INTRODUCTION

Free surface cusps appear widely in viscous flow problems [2] whenever the flow is strongly forced in an approximately two-dimensional manner, and such that viscous forces are comparable to surface tension forces. This balance is quantified by the dimensionless capillary number $\mathrm{Ca} = U\eta/\gamma$ being of order unity or larger, where U is a typical flow speed, η the fluid viscosity, and γ the coefficient of surface tension. On the right of Fig. 1 we show a cusp with a rounded tip, as found from a local analysis of Jeong and Moffatt's exact solution [1], and whose curvature increases exponentially with capillary number. The goal of this paper is to derive this structure directly from a local analysis of Stokes' equation.

Cusps have been demonstrated experimentally in a variety of geometries, for example by dragging fluid with two rollers [1, 3] or a single roller [4], or by pouring a jet of viscous liquid into a bath of the same liquid [5–7]. Theoretically, exact solutions of the two-dimensional Stokes equation showing cusping have been found by placing singularities underneath a free surface [1, 8–10], or next to a two-dimensional "drop" [11, 12].

Free-surface cusps deserve particular interest since they can serve as channels through which air can enter into a fluid, as shown theoretically [5, 6] and experimentally [4, 6]. It is important to distinguish cusps, which are quasi-two-dimensional objects, and which become singular along a line, from conical tips, which form at the end of bubbles in a variety of flows [13–15], and which become singular at a point. Available experimental evidence indicates that cusps occur when the driving flow becomes sufficiently two-dimensional, for example when a rising bubble is close to a wall. It is also known that a sufficiently large bubble rising in a *viscoelastic* liquid breaks axisymmetry to form a "knife-edge" ending in a cusp at its rear [16].

Most of the theoretical information we have about the structure of cusps comes from an analysis of exact solutions, found by mapping the fluid domain onto the unit disk. A cusp singularity of the free surface occurs when the map

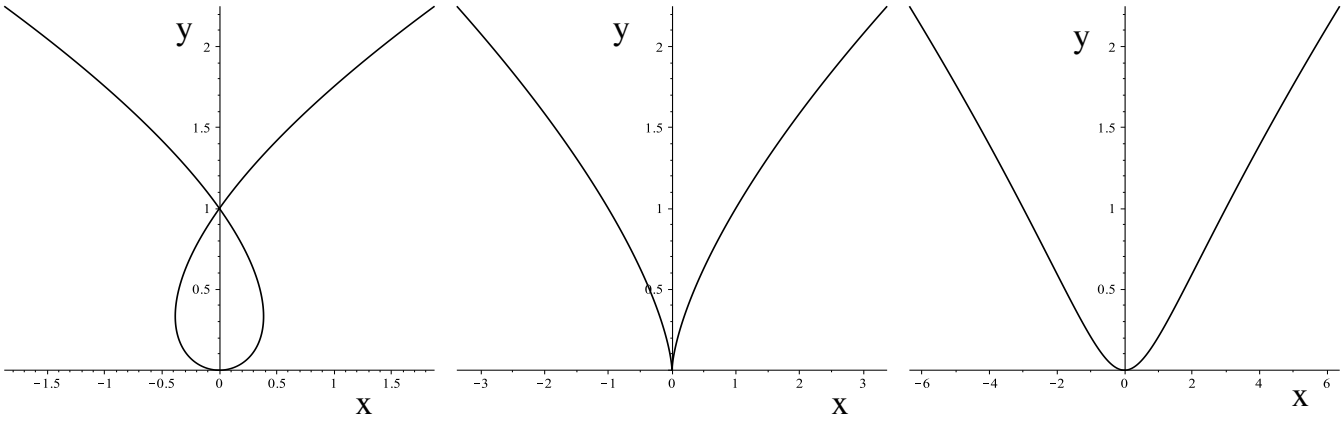

FIG. 1: A cusp can be understood as arising when a loop in a smooth curve is formed. We plot $x = \delta\varphi + c\varphi^3/3$, $y = \varphi^2/2$, for $c = 1$. On the left, $\delta < 0$, and the curve self-intersects, so the mapping is no longer invertible. In the middle, the critical state of $\delta = 0$ is shown, for which the curve is a cusp $x \propto y^{3/2}$. On the right, $\delta > 0$, and the curve has opened to produce a cusp in the far field, but being rounded at the tip. Physically, a cusp at finite capillary number corresponds to a rounded tip, whose curvature increases exponentially with the capillary number [1]. Thus formally the singular cusp in the middle occurs in the limit of infinite capillary number.

becomes non-invertible on the unit circle, corresponding to the free surface. This means the viscous cusp singularity has a very simple, highly universal structure, associated with an exponent of 3/2, when the width of the cusp is plotted as a function of the distance from the tip [17, 18]. Other physical examples, which share the self-similar structure with viscous cusps, appear in elasticity (the Hertz solution [19] and elastic folds [20]), biology [21], optics [22], relativistic membranes [23], shock formation [24], and contact line motion [25].

However, although the surface shape follows from simple geometrical considerations and is thus common to many different problems, the underlying physics, and in particular the underlying bulk motion away from the interface, is non-trivial, and can be quite different from problem to problem. It therefore remains to be shown for each individual case that the cusp structure follows from the equations of motion. It is this we will undertake in this paper for the case of Stokes' equation with a free surface.

A first step in this direction was taken in [3], where the 3/2 power law form of the cusp was calculated by a local expansion of Stokes' equation. However, this leaves open the structure of the tip, which is an important issue, since a truly singular tip would lead to a force singularity, which would produce a logarithmically infinite energy dissipation [3]. This issue was resolved by Jeong and Moffatt in [1], who showed that in their exact solution the tip was rounded on a scale exponentially small in the capillary number, making the energy dissipation finite.

As the starting point of our calculation we now derive the asymptotic form of the free surface shape of a cusp based on the idea that the parametric form of the curve $(x(\varphi), y(\varphi))$ is no longer invertible. This is motivated by Jeong and Moffatt's analysis, who for a free surface flow forced by a vortex dipole, find a smooth mapping $z = w(\zeta)$ of the unit disk onto the flow domain. A cusp singularity occurs when a point with $w'(\zeta) = 0$ approaches the unit circle from the outside. In terms of the parametric representation, such a singularity corresponds to $x'(\varphi) = y'(\varphi)) = 0$ [18] somewhere on the curve. The simplest, generic form of this singularity occurring at $\varphi = 0$ is (after appropriate rotations and rescaling) $x = c\varphi^3/3$ and $y = \varphi^2/2$, which reproduces the expected 3/2 scaling; the cusp has been oriented in the positive y-direction. The constant c provides a scale for the width of the cusp, and is a non-universal quantity depending on each individual flow configuration, as we will see below.

The generic perturbation to this singular shape (all other perturbations can again be eliminated by trivial transformations [2]) is $x = \delta\varphi + c\varphi^3/3$, $y = \varphi^2/2$, as shown in Fig. 1. For $\delta > 0$ this yields a rounded tip, as shown on the right of Fig. 1, for $\delta < 0$ the figure self-intersects, while for $\delta = 0$ the singular cusp is seen.

For the purposes of our calculation, we expand in the size $\kappa^{-1} \equiv \epsilon^2$ of the cusp tip, where κ is the curvature at the tip, written in suitable units of length. In the example presented by Jeong and Moffatt, this would be the distance of the singularity driving the flow from the free surface. With these conventions, the cusp solution becomes

$$x = \epsilon^2 \left(\psi + \epsilon c\psi^3/3\right), \quad y = \epsilon^2\psi^2/2, \tag{1}$$

which has a curvature $d^2y/dx^2 = y''/x'^2 = \epsilon^{-2} = \kappa$ at the tip, as required.

In the scaling of (1), taking the limit $\epsilon \to 0$ at constant ψ yields the tip region of the cusp, described by $x = \epsilon^2 y/2$. On the other hand, putting $\psi = \sigma/\sqrt{\epsilon}$, we obtain

$$x = \epsilon^{3/2} \left(\sigma + c\sigma^3/3\right), \quad y = \epsilon\sigma^2/2, \tag{2}$$

which has the form of a similarity solution. Exactly the same form of solution is obtained from the exact solution [1], for a particular value of c. We conclude that there are three relevant scales in our problem, as sketched in Fig. 2. In (1), ψ-values O(1) describe the tip, whereas σ-values O(1) describe the cusp. Finally, there is a non-universal outer length scale.

The purpose of this paper is to show that the full selfsimilar solution (1) or (2), written in units of the curvature and with c a free parameter, satisfies Stokes' equation. This is done using the boundary integral method, which involves integrals over the interface. To this end we still need to find the tangential velocity along the interface, which we do by calculating the limiting behavior of the exact solution found by Jeong and Moffatt on the inner and intermediate scales.

We will see that in the limit $\epsilon \to 0$ the integral equation splits into closed sets of equations on two different scales: the tip (inner) and the cusp (intermediate) scale. At the tip scale, the integral equation closes, so (1) is only needed in the tip region. At the cusp scale, the integrals have contributions from the tip, and more local contributions from the cusp itself.

In the next section II, we set up the integral equation and find the velocity. In the following sections III and IV, we calculate the limits of the boundary integral equation appropriate for the tip and cusp regions, respectively. For both regions, we then show that (1) is a solution.

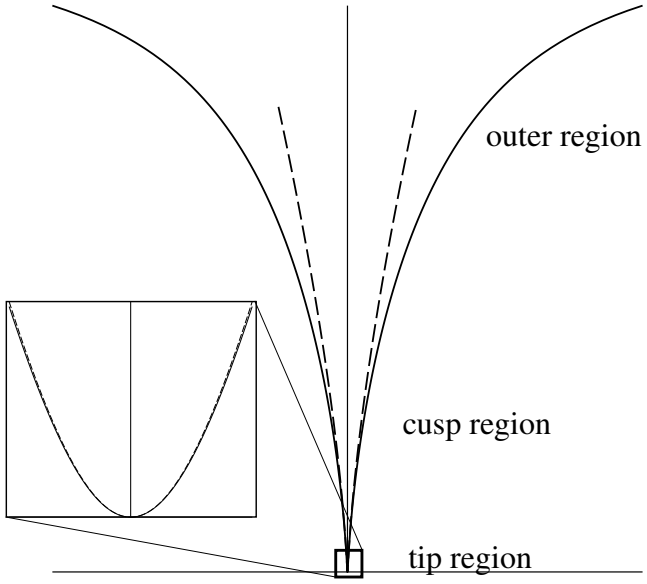

FIG. 2: A sketch of the scaling regions relevant for our calculations; the solid line is the exact solution of Jeong and Moffatt [1], the dashed line is (1), with $c = 3^{3/2}/4$ to fit the Jeong-Moffatt solution (cf. Appendix A). The inner tip region is the scale on which the tip is rounded, and is found keeping $\psi = O(1)$ as $\epsilon \to 0$ in (1). The intermediate cusp region is described by (2), and is recovered keeping σ constant. Finally, the outer solution depends on the particular problem at hand, and is found for $\psi = \phi/\epsilon$, where ϕ is held fixed.

II. THE INTEGRAL EQUATION

Boundary integral equations [26, 27] can be used to describe Stokes (viscously dominated) flow for an arbitrary combination of solid and free surfaces. The advantage is that they require information about the bounding surfaces only, in the case of a free surface (such as a bubble in an external flow) the value of the velocity field on the surface. While boundary integral equations have been used primarily for numerical purposes, here, following [15, 28], they are the starting point for an analytical treatment. The key idea is to make use of insight into the structure of the free surface, in order to write the boundary integral as an ordinary one-dimensional integral.

Since we are interested in a small neighborhood around a free-surface cusp only, here we restrict ourselves to the integral equation for a single free surface, which in units of $v_\eta = \gamma/\eta$ reads [29]

$$\frac{\mathbf{v}(\psi_1)}{2} = -\int_{-\infty}^{\infty} \kappa \mathbf{J}\cdot\hat{\mathbf{n}}\mathrm{d}\psi_2 - \int_{-\infty}^{\infty} \mathbf{v}\cdot\mathbf{K}\cdot\hat{\mathbf{n}}\mathrm{d}\psi_2 + \mathbf{v}^{(ext)}(\psi_1), \tag{3}$$

where ψ is used to parameterize the interface as $\mathbf{x}(\psi)$, and $\mathbf{v}(\psi)$ is a shorthand for $\mathbf{v}(\mathbf{x}(\psi))$. For convenience, we have written the boundary integral as an integral over the real line, and we assume that the surface can be closed at infinity in order to produce a closed surface, as required by the boundary integral method. The vector $\hat{\mathbf{n}} = (y_\psi, -x_\psi)$ points in the direction of the outward normal; with this choice, the parameter ψ used as integration variable is arbitrary.

In (3), defining $\mathbf{r} = \mathbf{x}_1 - \mathbf{x}_2$ and $r = |\mathbf{r}|$, kernels are defined by

$$\mathbf{J}(\mathbf{r}) = \frac{1}{4\pi}\left[-\mathbf{I}\ln r + \frac{\mathbf{rr}}{r^2}\right], \qquad \mathbf{K}(\mathbf{r}) = -\frac{1}{\pi}\frac{\mathbf{rrr}}{r^4}, \tag{4}$$

which are the Green functions of the two-dimensional Stokes equation. This means that $\mathbf{J}\cdot\mathbf{F}$ is the velocity generated at $\mathbf{x}_1$ by a point force $\mathbf{f} = \mathbf{F}\delta(\mathbf{x}_1 - \mathbf{x}_2)$, located at $\mathbf{x}_2$ (the "Stokeslet"), while $\mathbf{K}\cdot\mathbf{F}$ is the stress (the "stresslet"), and

$$\kappa = \frac{x_\psi y_{\psi\psi} - y_\psi x_{\psi\psi}}{\left(x_\psi^2 + y_\psi^2\right)^{3/2}}$$

is the curvature. The contribution $\mathbf{v}^{(ext)}$ is an externally applied velocity, which depends on the problem, and which does not affect the local structure of the solution. In the solution of [1] it is a vortex dipole, placed underneath the free surface. More generally, one can think of $\mathbf{v}^{(ext)}$ as the flow generated by all the stresses not represented by the first integral in (3), expanded to leading (monopole) order around the position of the cusp.

We are looking for *stationary* solutions, which implies that the interface is a streamline. Consequently, the velocity along the interface can be written

$$\mathbf{v} = u_0 \mathbf{t}, \quad \mathbf{t} = \frac{(x_\psi, y_\psi)}{\sqrt{x_\psi^2 + y_\psi^2}}, \tag{5}$$

with $\mathbf{t}$ the (normalized) tangent vector. The mathematical problem to be solved in this paper consists in solving the simultaneous equations (3) and (5) for an interface shape $\mathbf{x}(\psi)$, as well as for the tangential velocity $u_0(\psi)$.

We aim to solve (3) in the limit $\epsilon \to 0$. The most obvious strategy would be to rewrite (3) in terms of the similarity variable σ of (2). However, expanding κ at constant σ yields

$$\kappa = \epsilon^{-1/2} \frac{1 - 2c\sigma^2}{\sigma} + O(\epsilon^{3/2}),$$

which is singular at the tip as $\sigma \to 0$. Instead, we must resolve the interface on scale ψ, for which

$$\kappa = \frac{\epsilon^{-2}}{(1+\psi^2)^{3/2}}$$

as $\epsilon \to 0$, which is now regular for arbitrary ψ, up to an overall scale factor ϵ^{-2}.

Thus we solve (3) in two steps: first we solve for the flow near the tip, by taking the limit $\epsilon \to 0$ at constant ψ_1. Since the integral extends over all scales, we must consider ψ_2 varying over all scales. However, our analysis reveals that to leading order, all contributions (apart from constants), come from a region of $O(1)$ in ψ_2. In particular, the constant c does not come into play at this order, since its contribution in (1) is of higher order in ϵ. To find the tangential velocity u_0 on this scale, we can analyze the Jeong-Moffatt solution, as explained in more detail in Appendix A 2. Starting from (A4), putting $\theta = \pi/2 - \sqrt{3}\epsilon\psi$, and taking the limit $\epsilon \to 0$, using the approximation (A5), one finds

$$u_0(\psi) = -\frac{1}{\pi} \mathrm{arcsinh}\,(\psi) = -\frac{1}{\pi} \ln\left(\sqrt{1+\psi^2} + \psi\right) \tag{6}$$

to leading order in ϵ. In Section III below we confirm that (6), together with $x = \epsilon^2\psi$, $y = \epsilon^2\psi^2/2$, is a solution of the integral equation (3), to leading order $O(1)$ in ϵ.

In order to characterize the cusp, in Section IV we put $\psi = \sigma/\sqrt{\epsilon}$ and take the limit $\epsilon \to 0$ at constant σ. Analyzing the integral over ψ_2, in addition to the tip region the contributions now come from $\psi_2 = \sigma_2/\sqrt{\epsilon}$, where $\sigma_2 = O(1)$. To leading order, the tangential velocity (6) is now

$$u_0 = \frac{1}{2\pi} \ln\left(\frac{\epsilon}{4\sigma^2}\right), \tag{7}$$

and the interface is given by (2), with arbitrary c. The dependence of u_0 on σ, $u_0 \sim -\ln(\sigma)/\pi$, corresponds to the flow generated by an upward force of strength 2γ, located at the tip of the cusp, as suggested by J. Hinch, see the appendix to [1].

III. THE TIP REGION

To investigate the tip, we hold ψ_1 constant and let $\epsilon \to 0$; the interface is described by (1). We obtain for the left hand side of (3):

$$\frac{\mathbf{v}}{2} = u_0(\psi_1) \frac{(1, \psi_1)}{2\sqrt{1+\psi_1^2}}, \tag{8}$$

so for both components, the leading order is $O(\epsilon^0)$. Expanding the integrand $f \equiv \kappa \mathbf{J} \cdot \hat{\mathbf{n}}|_{x/y}$ into a power series in ϵ (and similarly for the K-integral in (3)), we obtain an *inner* expansion

$$f \approx \sum_{n=0}^{Q} f_n(\psi_2) \epsilon^n \equiv I_Q f, \tag{9}$$

using the notation of e.g. [30].

However, the integrals over $f_1(\psi_2)$ (as well as higher-order coefficients) are divergent for $\psi_2 \to \infty$, indicating a non-uniform behavior of the integrand as $\epsilon \to 0$. Thus we have to combine (9) with an *outer* expansion [31]

$$f \approx \sum_{n=1}^{Q+1} F_n^{\pm}(\phi_2)\epsilon^n \equiv O_{Q+1} f, \tag{10}$$

where now $\psi_2 = \phi_2/\epsilon$, with ϕ_2 held constant. In the outer expansion, we have to go to higher order than in (9), in order to guarantee a contribution of the same order to the integral, considering that the integration variable is now ϕ instead of ψ. The two signs $\pm$ correspond to expansions for $\phi_2 > 0$ and $\phi_2 < 0$, respectively. Since ψ_1 only appears in the combination $\psi_2 - \psi_1 = \phi_2/\epsilon - \psi_1$, the leading order contribution $F_1^{\pm}(\phi_2)$ is independent of ψ_1.

From the two expansions (9) and (10) one can construct a composite solution $f \approx I_Q f + O_{Q+1} f - I_Q O_{Q+1} f$, using that $I_Q O_{Q+1} f = O_{Q+1} I_Q f$ [32]. Since we only want to solve (3) to leading order $O(\epsilon^0)$, we only have to consider the case $Q = 0$; it turns out that the overlap integral $O_1 I_0 f$ vanishes for both components of the J and K integrals, so we compute

$$\int_{-\infty}^{\infty} f(\psi_2, \epsilon) d\psi_2 \approx \int_{-\infty}^{\infty} f_0(\psi_2) d\psi_2 + \int_{-\infty}^{0} F_1^{-}(\phi_2) d\phi_2 + \int_{0}^{\infty} F_1^{+}(\phi_2) d\phi_2, \tag{11}$$

remembering that $d\phi_2 = \epsilon d\psi_2$, so both inner and outer expansions contribute at leading order. However, the outer expansion only contributes a ψ_1-independent constant (which vanishes for the x-component), but which only sets the curvature $\kappa = \epsilon^{-2}$ as we will see. Also note that the outer solution (scale ϕ_2) is no longer universal, but depends on the individual problem. In other words, on the tip scale we have

$$\frac{u_0(\psi_1)}{2\sqrt{1+\psi_1^2}} = -J_x^{(in)}(\psi_1) - K_x^{(in)}(\psi_1) \tag{12}$$

$$\frac{u_0(\psi_1)\psi_1}{2\sqrt{1+\psi_1^2}} = -J_y^{(in)}(\psi_1) - K_y^{(in)}(\psi_1) + J_y^{(in)}(0) + K_y^{(in)}(0), \tag{13}$$

where in (13) we have subtracted the integrals for $\psi_1 = 0$, so the aforementioned constants drop out, and both sides vanish for $\psi_1 = 0$. The superscript (in) refers to the integral over the inner expansion, the first integral on the right of (11).

The important insight of our asymptotic analysis so far is that in the limit $\epsilon \to 0$, the boundary integral equation (3) reduces to a closed equation for the tip of the cusp, of size $\kappa^{-1} = \epsilon^2$. The inner expansion (12),(13) does not contain any parameters, and is thus guaranteed to be satisfied by virtue of the global exact solution [1]. In Appendix B 1, we have confirmed this result by evaluating the integrals appearing in (12) for any ψ_1. This establishes that a tip of the form $y = x^2/(2\epsilon^2)$, together with the tangential velocity (6), is a universal feature of any sharp tip in viscous two-dimensional Stokes flow, regardless of the geometry or external driving.

Addressing the constants appearing in (13), which have been subtracted, we evaluate the y-component of (3) at $\psi_1 = 0$, which for $\epsilon \to 0$ has the form

$$v^{(ext)}(0) = J_y^{(in)}(0) + K_y^{(in)}(0) + J_y^{(out)}(0) + K_y^{(out)}(0), \tag{14}$$

where the superscript (out) refers to the integral over the outer expansion, the second and third integrals on the right of (11). In Appendix B 2 we show, using Jeong and Moffatt's exact solution, that (14) is indeed satisfied exactly. In order to achieve this result, contributions from the entire interface, from a region of size $O(1)$ and beyond, must be taken into account.

In particular, using a definition of Ca in terms of the external flow, the relation between Ca and the tip curvature is non-universal and depends on properties of the entire solution. For example, one could *define* the capillary number as the y-component of the external velocity $\mathrm{Ca} = v^{(ext)}(0)$ (in units of the capillary speed), evaluated at the position of the cusp. If now the integrals on the right of (14) are of the form $a + b \ln \epsilon$, and remembering that $\epsilon = \sqrt{\kappa}$ in units of the distance between free surface and the dipole, one obtains

$$\kappa = e^{2a/b} e^{-2\mathrm{Ca}/b}. \tag{15}$$

Thus one finds exponential growth of the curvature [1], but the coefficients are not universal. In the particular case treated in [1], one finds (cf. (B8))

$$a = \frac{9}{16\pi} \ln \frac{\sqrt{3}}{16}, \quad b = \frac{9}{16\pi},$$

so that

$$\kappa_{JM} = \frac{3}{256} e^{-32\pi \mathrm{Ca}/9}.$$

This is different from, but of course equivalent to the relation derived in [1], where the definition of Ca was based on the strength of the driving vortex dipole and its distance from the unperturbed interface.

IV. THE CUSP REGION

The above calculation on the scale of the tip only applies to the inner region for which $\psi = O(1)$, where in the limit $\epsilon \to 0$, $y = x^2\kappa/2$. Now we turn to the scale of the cusp, for which $\psi = \sigma/\sqrt{\epsilon}$ in (1), with σ fixed as ϵ goes to zero. We will see that evaluating J and K integrals requires different approximations, so we treat them separately.

A. J-integrals

The J-integrals can be evaluated in a similar fashion to that of the tip scale, but on account of the scaling $\psi = \sigma/\sqrt{\epsilon}$, we now expand in powers of $\sqrt{\epsilon}$. To represent the integrand to a required order, in addition to the previous inner and outer regions, we require a third intermediate region, so that the three different regions are defined on scales ψ_2 (inner), $\psi_2 = \sigma/\sqrt{\epsilon}$ (intermediate), and $\psi_2 = \phi/\epsilon$ (outer).

Thus if f is the integrand, we consider three different expansions in order to represent the integral to a given order:

$$f \approx \sum_{n=0}^{Q-1} f_n(\psi_2)\epsilon^{n/2} \equiv I_{Q-1}f, \quad f \approx \sum_{n=1}^{Q} \overline{f}_n(\sigma)\epsilon^{n/2} \equiv M_Q f, \quad f \approx \sum_{n=2}^{Q+1} F_n(\phi)\epsilon^{n/2} \equiv O_{Q+1}f.$$

The outer expansion is not universal, and therefore cannot be computed from the universal cusp solution. Note however, that it only contributes a constant, and therefore does not need to be considered, except for the calculation of κ.

We can now define inner and outer composite solutions by proceeding in two steps. First we construct two composite solutions using the inner and intermediate expansions, and the intermediate and outer expansions, respectively, which results in the intermediate composite solutions

$$I_{Q-1}f + M_Q f - I_{Q-1}M_Q f \equiv I_c f, \quad M_Q f + O_{Q+1}f - M_Q O_{Q+1} f \equiv O_c f. \tag{16}$$

The resulting two expansions are then combined to find a composite solution for the integral I valid everywhere:

$$I \approx I_c f + O_c f - M_Q I_c f, \tag{17}$$

where $M_Q I_c f = M_Q O_c f$, to any order of $\sqrt{\epsilon}$, set by Q.

Beginning with the left hand side of (3),

$$\frac{\mathbf{v}}{2} = \frac{1}{4\pi} \ln\left(\frac{\epsilon}{4\sigma_1^2}\right) \left(\frac{1 + c\sigma_1^2}{\sigma_1}\sqrt{\epsilon} + O(\epsilon^{3/2}), 1 + O(\epsilon) \right), \tag{18}$$

so we need the x-component to $O(\sqrt{\epsilon})$ and the y-component to $O(1)$. Analysis of the composite solution for the integrand of the J-integral shows that the leading order $O(1)$ contribution cancels owing to symmetry; at the next order $O(\sqrt{\epsilon})$, only $I_{Q-1}f$ contributes to the composite solution with $Q = 2$. This yields (with corrections of $O(\epsilon)$)

$$\int_{-\infty}^{\infty} \kappa \mathbf{J} \cdot \hat{\mathbf{n}}|_x \, d\psi_2 = \int_{-\infty}^{\infty} I_1 f \, d\psi_2 = -\sqrt{\epsilon} \frac{1 + c\sigma_1^2/3}{2\pi\sigma_1} \int_{-\infty}^{\infty} \frac{d\psi_2}{(1+\psi_2^2)^{3/2}} = -\sqrt{\epsilon} \frac{1 + c\sigma_1^2/3}{\pi\sigma_1}. \tag{19}$$

As for the y-component of the J-integral, the only contributions are from the inner and the outer expansions. This yields, putting $Q = 1$,

$$\int_{-\infty}^{\infty} \kappa \mathbf{J} \cdot \hat{\mathbf{n}}|_y \, d\psi_2 = \int_{-\infty}^{\infty} I_0 f \, d\psi_2 + \int_{-\infty}^{0} O_1^- f \, d\phi_2 + \int_{0}^{\infty} O_1^+ f \, d\phi_2 + O(\sqrt{\epsilon}).$$

Here the outer expansion only contributes a (σ_1-independent) constant, which is not universal. In fact, since the cusp scale is much smaller than the outer length scale, the outer contributions must be exactly the same as those found for the tip region. Thus performing the inner integral, we find

$$\int_{-\infty}^{\infty} \kappa \mathbf{J}\cdot\hat{\mathbf{n}}|_y \, d\psi_2 = \frac{1}{4\pi}\left(\ln\left(\frac{\epsilon\sigma_1^2}{2}\right)-1\right)\int_{-\infty}^{\infty}\frac{d\psi_2}{(1+\psi_2^2)^{3/2}} = \frac{1}{2\pi}\left(\ln\left(\frac{\epsilon\sigma_1^2}{2}\right)-1\right) + J_y^{(out)}(0), \tag{20}$$

where $J_y^{(out)}(0)$ has been calculated in Appendix (B 2) for the case of the Jeong-Moffatt solution.

B. K-integrals

To compute the x and y components of the K-integral, another asymptotic region has to be considered, which comes from the factor r^4 in the denominator of the K-integral (cf. (4)), becoming small as a function of ψ_2. Using (1) one finds $r^2 = (\psi_1-\psi_2)^2\epsilon^4 D/9$, where

$$D = c^2(\psi_1^2+\psi_1\psi_2+\psi_2^2)^2\epsilon^2 + 6c(\psi_1^2+\psi_1\psi_2+\psi_2^2)\epsilon + 9\psi_1^2/4 + 9\psi_2\psi_1/2 + 9\psi_2^2/4 + 9.$$

The factor $(\psi_1-\psi_2)^2$ in r^2 comes from the "local" contribution, where the integration variable equals the position along the interface where the velocity is computed. This does not lead to a singularity, since at the same point $\hat{\mathbf{n}}\cdot\mathbf{r}\sim(\psi_1-\psi_2)^2$, $\mathbf{t}\cdot\mathbf{r}\sim\psi_1-\psi_2$, and $\mathbf{r}\sim\psi_1-\psi_2$, so the zeroes of numerator and denominator of the integrand cancel.

Instead, the main contribution to the K-integral comes from a region of size $\Delta\psi_2 = O(1)$ around the minimum of D, instead of around the origin; the location of the minimum we denote by ψ_m. Putting $\psi_1 = \sigma_1/\sqrt{\epsilon}$, ψ_m is found from $dD/d\psi_2 = 0$. To leading order as $\epsilon\to 0$ this yields $9(\sigma_1/\sqrt{\epsilon}+\psi_2)/2 = 0$, so that $\psi_m = -\sigma_1/\sqrt{\epsilon}+O(\sqrt{\epsilon})$. To perform the integrals, we write the integrand IK of the K-integral in the form $IK = N/D^2$. This means that putting $\Delta = \psi_2-\psi_m$, we can expand the integrand in the form:

$$IK = \frac{N}{D^2}, \quad D = D_0 + \frac{\Delta^2}{D_m} + O(\Delta^3). \tag{21}$$

From the definition of D, the functions D_0, D_m, and ψ_m can now be calculated in a power series in ϵ. Higher powers in Δ contribute a sub-leading contribution to the integral. Specifically, solving $dD/d\psi_2 = 0$ iteratively, we find

$$\psi_m = -\frac{\sigma_1}{\sqrt{\epsilon}} + \frac{4c\sigma_1}{9}s\sqrt{\epsilon} + O(\epsilon^{3/2}).$$

Neglecting contributions of order ϵ, we find (using the abbreviation $s = 3+c\sigma_1^2$) $D_0 = s^2+O(\epsilon)$, and $D_m = 4/9+O(\epsilon)$.

Beginning with the x-component of the K-integral, the numerator can be expanded as $N(\psi_m+\Delta) = N_0(\Delta) + N_1(\Delta)\sqrt{\epsilon}+\ldots$, where N_0 is linear in Δ, and therefore gives a vanishing contribution. The next order in $\sqrt{\epsilon}$ is

$$N_1 = \frac{s^4}{2\pi^2\sigma_1}\ln\left(\frac{2\sigma_1}{\sqrt{\epsilon}}\right) + \frac{9s}{4\pi^2\sigma_1}\left[c\sigma_1^2\ln\left(\frac{2\sigma_1}{\sqrt{\epsilon}}\right)+s\right]\Delta^2,$$

so that using

$$\int_{-\infty}^{\infty}\frac{d\Delta}{D^2} = \frac{\pi}{3s^3}, \quad \int_{-\infty}^{\infty}\frac{\Delta^2 d\Delta}{D^2} = \frac{4\pi}{27s},$$

we obtain

$$\int_{-\infty}^{\infty}\mathbf{v}\cdot\mathbf{K}\cdot\hat{\mathbf{n}}|_x\, d\psi_2 \approx \sqrt{\epsilon}\int_{-\infty}^{\infty}\frac{N_1(\Delta)}{\left(D_0+\Delta^2/D_m\right)^2}d\Delta = \left[\frac{1+c\sigma_1^2/3}{\pi\sigma_1} + \frac{1+c\sigma_1^2}{2\pi\sigma_1}\ln\left(\frac{2\sigma_1}{\sqrt{\epsilon}}\right)\right]\sqrt{\epsilon}. \tag{22}$$

To check the size of the remainder, we expand

$$\mathbf{v}\cdot\mathbf{K}\cdot\hat{\mathbf{n}}|_x - \frac{N_1}{D^2}\sqrt{\epsilon}$$

in ϵ, using the outer scale $\psi_2 = \phi_2/\epsilon$. The first non-vanishing contribution to this remainder is of order $\epsilon^{5/2}$, and thus sub-dominant.

In the same way, one can calculate the dominant contribution to the y-component of the K-integral, which is of the form (21), but with

$$N = N_0(\Delta) + O(\sqrt{\epsilon}) = -\frac{27s}{8\pi^2} \ln\left(\frac{2\sigma_1}{\sqrt{\epsilon}}\right),$$

so now we have

$$\int_{-\infty}^{\infty} \mathbf{v}\cdot\mathbf{K}\cdot\hat{\mathbf{n}}|_y \, d\psi_2 \approx \int_{-\infty}^{\infty} \frac{N_0(\Delta)}{\left(D_0 + \Delta^2/D_m\right)^2} d\Delta = \frac{1}{2\pi} \ln\left(\frac{\sqrt{\epsilon}}{2\sigma_1}\right) + K_y^{(out)}(0). \tag{23}$$

As before, the outer contribution to the integral on scale ϕ_2/ϵ must be the same as that for the cusp expansion of Section IV. This constant $K_y^{(out)}(0)$ has been calculated in Appendix B 2 for the special case of the Jeong-Moffatt geometry.

We can now verify that the interface shape (2), together with the tangential velocity (7), satisfies the integral equation (3) on the scale of the cusp. In the limit $\epsilon \to 0$ the external flow is once more

$$\mathbf{v}^{(ext)} = \left(O(\epsilon^{3/2}), \frac{9}{16\pi} \ln\frac{\sqrt{3}\epsilon}{16} + O(\epsilon)\right). \tag{24}$$

Thus for the x-component we have using (18), (19), and (22) that

$$\frac{1}{4\pi} \ln\left(\frac{\epsilon}{4\sigma_1^2}\right) \frac{1 + c\sigma_1^2}{\sigma_1}\sqrt{\epsilon} = \sqrt{\epsilon}\frac{1 + c\sigma_1^2/3}{\pi\sigma_1} - \left[\frac{1 + c\sigma_1^2/3}{\pi\sigma_1} + \frac{1 + c\sigma_1^2}{2\pi\sigma_1} \ln\left(\frac{2\sigma_1}{\sqrt{\epsilon}}\right)\right]\sqrt{\epsilon},$$

which is satisfied for *any* c. This confirms that locally the cusp is determined up to a free constant c only, which then is set by the external flow and the boundary conditions.

As for the y-component, the corresponding balance is, using (18), (20), and (23), that

$$\frac{1}{4\pi} \ln\left(\frac{\epsilon}{4\sigma_1^2}\right) = -\frac{1}{2\pi}\left(\ln\left(\frac{\epsilon\sigma_1^2}{2}\right) - 1\right) - J_y^{(out)}(0) - \frac{1}{2\pi} \ln\left(\frac{\sqrt{\epsilon}}{2\sigma_1}\right) - K_y^{(out)}(0) + \frac{9}{16\pi} \ln\frac{\sqrt{3}\epsilon}{16}.$$

It is easy to check that the universal dependence on σ_1, which comes from the inner contribution to the integrals, is satisfied identically. The remaining constant is not universal, but it is easily confirmed that with the constants calculated in Appendix B 2, the equation is satisfied identically for the Jeong-Moffatt geometry.

V. CONCLUSIONS

In conclusion, we have shown that two-dimensional flows exhibiting free-surface cusps in the limit of strong driving, previously found using exact methods, have a universal structure that applies to any flow geometry. The curvature of the tip of the cusp grows exponentially with the strength of the driving, but involving coefficients which are not universal and which depend on features of the flow over all scales.

The advantage of having a local solution is that it may serve as a building block of a more complicated solution, for example containing several singularities, or existing in dimensions higher than two. As concerns the first possibility, out of two cusp singularities, a singularity of higher order can be constructed [18], which we expect can be shown to be a solution of free-surface Stokes flow using the same method as used here. As for higher dimensions, in practice no flow will be exactly two-dimensional. Instead, the flow intensity may vary in the third direction along the cusp line, as a result of which the two-dimensional solution "unfolds" [2] into the third dimension.

Another interesting question concerns the transition between two-dimensional cusps (treated here), and three-dimensional, near conical tips [28], which one should be able to address with an understanding of the local cusp solution.

Appendix A: The Jeong-Moffatt solution

1. The free surface

In the exact solution of [1], the free surface is given by the complex mapping

$$w(\zeta) = a(\zeta + i) + (a + 1)i\frac{\zeta - i}{\zeta + i}, \tag{A1}$$

where $\zeta = e^{i\theta}$. Taking the real and imaginary parts yields

$$x = a\cos\theta + \frac{(a+1)\cos\theta}{1+\sin\theta}, \quad y = a(\sin\theta - 1), \tag{A2}$$

where the y-coordinate has been shifted so that $(x, y) = (0, 0)$ at the cusp $\theta = \pi/2$. Putting $a = -1/3 + \bar{\epsilon}$, where $\bar{\epsilon}$ is called ϵ in the notation of [1], the singularity is reached for $\bar{\epsilon} \to 0$. The mapping (A2) first becomes non-invertible for $\theta = \pi/2$, so to describe the neighborhood of the cusp, we put $\theta = \pi/2 - \varphi$ and expand in φ. Then the curvature, in units of the distance d between the double dipole and the free surface, is $\kappa = 4/(27\bar{\epsilon}^2)$; thus $\bar{\epsilon} = (2/\sqrt{27})\epsilon$.

Expanding in $\bar{\epsilon}$ and φ, where we take $\varphi = O(\sqrt{\bar{\epsilon}})$, we have

$$x = \frac{3\bar{\epsilon}}{2}\varphi + \frac{\varphi^3}{12}, \quad y = \frac{\varphi^2}{6}.$$

In order to bring that into the form (1), we substitute $\varphi = \sqrt{3}\epsilon\psi$, from which we find $c = 3^{3/2}/4$.

2. The tangential velocity

We use the exact solution to find the velocity field in the limit of vanishing ϵ, which we then demonstrate to be part of a local solution to the integral equation (3). Since the interface is stationary, we only need the tangential velocity u_0. According to [1], equation (3.11), if α is the dipole strength driving the flow, this is

$$u_0 = -\frac{\alpha}{H(a)}(1+\sin\theta)\cos\theta|w'(e^{i\theta})|I(\sin\theta; a), \tag{A3}$$

where ($a < 0$)

$$H = -\frac{a(3a+2)^2}{1+a+\sqrt{-2a(a+1)}}K(m)$$

and

$$I(\zeta; a) = \frac{4}{(t_1-\zeta)\left[a+1+\sqrt{-2a(a+1)}\right]}\left(K(m) - \frac{t1+1}{\zeta+1}\Pi(n,m)\right),$$

with

$$t_1 = \frac{-a(2a+1)+(a+1)\sqrt{-2a(a+1)}}{a(3a+2)}, \quad n = \frac{2(\zeta - t1)}{(\zeta+1)(1-t_1)}, \quad m = \frac{2}{\left(-\frac{2a}{a+1}\right)^{1/4} + \left(-\frac{a+1}{2a}\right)^{1/4}},$$

where $K(m)$ and $\Pi(n, m)$ are the usual elliptic integrals of the first and third kinds, respectively, as defined in [33]. According to [1], (2.38), $\alpha/v_\eta = H(a)/4\pi$, where $v_\eta = \gamma/\eta$ is the capillary velocity, and so in units of v_η:

$$u_0 = -\frac{1}{4\pi}(1+\sin\theta)\cos\theta|w'(e^{i\theta})|I(\sin\theta; a). \tag{A4}$$

For ζ real between -1 and 1, $\Pi(n, m)$ has to be interpreted as a principle value. To avoid this, we first express $\Pi(n, m)$ through

$$R_J(x, y, z, p) = \frac{3}{2}\int_0^\infty \frac{dt}{(t+p)\sqrt{(t+x)(t+y)(t+z)}},$$

as defined in [34], and then use the identity (6.11.21) of [34] to arrive at

$$\Pi(n, m) = K(m) + \frac{n}{3}R_j(0, 1-m^2, 1, 1-n) = \frac{m^2}{m^2-n}K(m) + \frac{nm^2(1-m^2)}{3(m^2-n)^2}R_j(0, q, 1, p),$$

where $q = 1 - m^2$ and $p = n(1-m^2)/(n-m^2) > 1$. To obtain an approximation to $\Pi(n,m)$ that is uniform in θ, we rescale and then split the integral into two pieces:

$$R_j(0,q,1,p) = \frac{3}{2}\int_0^\infty \frac{dt}{(t+p)\sqrt{t(t+q)(t+1)}} = \frac{3}{2q^{3/2}}\int_0^\infty \frac{ds}{(s+r)\sqrt{s(s+1)(s+q^{-1})}} = \frac{3}{2q^{3/2}}\left(\int_0^{q^{-1/2}} ds + \int_{q^{-1/2}}^\infty ds\right),$$

where $r = p/q = n/(n-m^2)$. Since $q = (3/16)\epsilon^2 + O(\epsilon^3)$, for $\epsilon \to 0$ we can make the uniform approximations $s + q^{-1} \approx q^{-1}$ in the first integral, and $s + 1 \approx s$ in the second, which results in integrals which can be performed analytically to give

$$R_j(0,q,1,p) \approx \frac{3}{2q} I_1(q^{-1/2}) + \frac{3}{2} I_2(q^{1/2}), \tag{A5}$$

where

$$I_1(s) = \frac{\operatorname{arccoth}\frac{2rs+r-s}{2\sqrt{r}\sqrt{r-1}\sqrt{s}\sqrt{s+1}}}{\sqrt{r}\sqrt{r-1}}, \quad I_2(t) = \frac{2\operatorname{arccoth}\frac{\sqrt{t+1}}{\sqrt{1-p}} + \ln\frac{\sqrt{t+1}-1}{\sqrt{t+1}+1}\sqrt{1-p}}{\sqrt{1-pp}}.$$

With these simplifications, we can now compute a series expansion of u_0 in ϵ at constant ψ; this yields (6) at leading order.

Appendix B: Calculation of integrals

1. Inner integrals

In the inner expansion, for the integrand of the J-integral we find to leading order in ϵ that

$$\kappa \mathbf{J}\cdot\hat{\mathbf{n}}\big|_x = -\frac{\psi_2}{8\pi\left(1+\psi_2^2\right)^{3/2}}\ln\left[\left((\psi_1+\psi_2)^2+4\right)(\psi_1-\psi_2)^2\right] + \frac{1}{2\pi}\frac{\psi_2-\psi_1}{\left(1+\psi_2^2\right)^{3/2}\left((\psi_1+\psi_2)^2+4\right)} + \frac{\psi_2\ln(2/\epsilon^2)}{4\pi\left(1+\psi_2^2\right)^{3/2}} \tag{B1}$$

and

$$\kappa \mathbf{J}\cdot\hat{\mathbf{n}}\big|_y = \frac{\ln(\epsilon^2/2)}{4\pi\left(1+\psi_2^2\right)^{3/2}} + \frac{\ln\left[\left((\psi_1+\psi_2)^2+4\right)(\psi_1-\psi_2)^2\right]}{8\pi\left(1+\psi_2^2\right)^{3/2}} + \frac{\psi_2^2-\psi_1^2}{4\pi\left(1+\psi_2^2\right)^{3/2}\left((\psi_1+\psi_2)^2+4\right)}. \tag{B2}$$

The K-integral, on the other hand, yields for the inner expansion:

$$\mathbf{v}\cdot\mathbf{K}\cdot\hat{\mathbf{n}}\big|_x = \frac{4u_0(\psi_2)}{\pi}\frac{\psi_2(\psi_1+\psi_2)+2}{\left(1+\psi_2^2\right)^{1/2}\left((\psi_1+\psi_2)^2+4\right)^2} \tag{B3}$$

and

$$\mathbf{v}\cdot\mathbf{K}\cdot\hat{\mathbf{n}}\big|_y = \frac{2u_0(\psi_2)}{\pi}\frac{(\psi_1+\psi_2)\left(\psi_2(\psi_1+\psi_2)+2\right)}{\left(1+\psi_2^2\right)^{1/2}\left((\psi_1+\psi_2)^2+4\right)^2}. \tag{B4}$$

We focus on verifying (12), (13) is treated similarly. To this end we split (12) up in the form

$$-\frac{\operatorname{arcsinh}(\psi_1)}{\sqrt{1+\psi_1^2}} = -J_{x1} + J_{x21} + J_{x22} + K_x, \tag{B5}$$

where

$$J_{x1} = \int_{-\infty}^\infty \frac{\psi_2-\psi_1}{\left(1+\psi_2^2\right)^{3/2}\left((\psi_1+\psi_2)^2+4\right)}d\psi_2, \quad J_{x21} = \int_{-\infty}^\infty \frac{\psi_2\ln\left((\psi_1+\psi_2)^2+4\right)}{4\left(1+\psi_2^2\right)^{3/2}}d\psi_2, \quad J_{x22} = \int_{-\infty}^\infty \frac{\psi_2\ln|\psi_1-\psi_2|}{2\left(1+\psi_2^2\right)^{3/2}}d\psi_2,$$

$$K_x = \int_{-\infty}^\infty \frac{8\operatorname{arcsinh}(\psi_2)}{\pi\sqrt{1+\psi_2^2}}\frac{\psi_2(\psi_1+\psi_2)+2}{\left((\psi_1+\psi_2)^2+4\right)^2}d\psi_2.$$

The contribution J_{x1} is of the form

$$\int \frac{P(x)}{Q(x)\sqrt{1+x^{2^n}}}dx, \tag{B6}$$

so that primitives can be found using a method described in [33]. We calculated the definite integral J_{x1} in terms of elementary functions, using MAPLE. The contributions from J_{x21} and J_{x22} are simplified integrating by parts, the result is

$$J_{x21} = \int_{-\infty}^{\infty} \frac{(\psi_1+\psi_2)}{2\left((\psi_1+\psi_2)^2+4\right)\sqrt{1+\psi_2^2}}d\psi_2,$$

which MAPLE integrates in terms of elementary functions. To calculate J_{x22}, we note

$$\int \frac{\psi_2 \ln|\psi_1-\psi_2|}{\left(1+\psi_2^2\right)^{3/2}}d\psi_2 = \int \frac{d\psi_2}{(\psi_2-\psi_1)\sqrt{1+\psi_2^2}} - \frac{\ln|\psi_1-\psi_2|}{\sqrt{1+\psi_2^2}} = -\frac{\operatorname{arcsinh}\frac{1+\psi_1\psi_2}{|\psi_1-\psi_2|}}{\sqrt{1+\psi_1}} - \frac{\ln|\psi_1-\psi_2|}{\sqrt{1+\psi_2^2}},$$

from which we find

$$J_{x22} = -\frac{\operatorname{arcsinh}\psi_1}{\sqrt{1+\psi_1^2}},$$

which cancels the left hand side of (B5).

Finally K_x, whose integrand has branch points at $z=\pm i$, can be simplified using contour integration. We choose branch cuts that extend from $\pm i$ to infinity along the imaginary axis, so that for $z=it$

$$\sqrt{1+z^2} = \pm i\sqrt{t^2-1}, \quad \operatorname{arcsinh}(z) = \frac{i\pi}{2} \pm \ln\left(\sqrt{t^2-1}+t\right),$$

to the right and left of the upper branch cut, respectively. Further, the integrand has a pole at $\psi_2 = 2i-\psi_1$. Thus choosing as the contour the real axis, plus a circle at infinity, avoiding the upper branch cut, one finds

$$K_x = -8\Im\left\{\int_1^{\infty} \frac{2+it(\psi_1+it)dt}{\sqrt{t^2-1}\left((\psi_1+it)^2+4\right)^2}\right\} - 2\pi\Im\left\{\operatorname{Res}(f,\psi_2=2i-\psi_1)\right\},$$

where $f(\psi_2)$ is the integrand of K_x.

The integral over t can again be performed in terms of elementary functions, using MAPLE, which shows that indeed

$$K_x = J_{x1} - J_{x21},$$

which demonstrates (B5) and thus (12).

2. Constants in the integral equation

In the y-component of the integral equation, (13), we have computed integrals up to constants only, since the constants depend on the particular problem at hand. However, as a test of our method, it is instructive to calculate all constants based on the exact solution [1], and to verify (14).

Beginning with the left hand side of (14), the external flow is

$$u - iv = -\frac{i\alpha}{(z+i)^2} = -v_\eta \frac{iH(a)}{4\pi(z+i)^2}, \quad H(a) \approx \ln(32/(9\bar{\epsilon}))/4 = \ln(16/(\sqrt{3}\epsilon))/4, \tag{B7}$$

and the tip of the cusp is at $z = 2ai = (-2/3+2\bar{\epsilon})i$. Thus to leading order, in units of v_η, the y-component of the external velocity is

$$v^{(ext)} = \frac{9}{16\pi}\left(\ln\epsilon + \ln\frac{\sqrt{3}}{16}\right). \tag{B8}$$

The integrals on the right of (14) go from $\varphi = -\pi$ to $\varphi = \pi$, so with $\theta = \pi/2 - \sqrt{3}\epsilon\psi$ and the inner/outer expansion $f(\psi_2) = f_0(\psi_2) + F_1(\phi_2)\epsilon$ we have

$$\int_{-\pi/(\sqrt{3}\epsilon)}^{\pi/(\sqrt{3}\epsilon)} f(\psi_2)d\psi_2 = \int_{-\pi/(\sqrt{3}\epsilon)}^{\pi/(\sqrt{3}\epsilon)} f_0(\psi_2)d\psi_2 + \int_{-\pi/(\sqrt{3}\epsilon)}^{\pi/(\sqrt{3}\epsilon)} F_1(\phi_2)d\psi_2 = \int_{-\infty}^{\infty} f_0(\psi_2)d\psi_2 + \int_{-\pi/\sqrt{3}}^{\pi/\sqrt{3}} F_1(\phi_2)d\phi_2,$$

having taken the limit $\epsilon \to 0$ and substituting $\psi_2 = \phi_2/\epsilon$ in the second step. The inner expansion f_0 for both J and K integrals is universal, and determined by the local cusp alone:

$$J_y^{(in)}(0) = -0.06130418454 + \ln\epsilon/\pi, \quad K_y^{(in)}(0) = -0.4288041588.$$

The actual expressions are prohibitively complicated, so we only give their numerical values.

To compute F_1, the full expressions for the shape, and (A4) for the tangential velocity, using the approximation (A5), are evaluated in the limit $\epsilon \to 0$ at constant ϕ. The results are

$$J_y^{(out)}(0) = 0.2112196778, \quad K_y^{(out)}(0) = -0.119188 - 7\ln\epsilon/(16\pi),$$

so that indeed (14) is satisfied, which can be checked numerically.

References

[1] J.-T. Jeong and H. K. Moffatt. Free-surface cusps associated with a flow at low Reynolds numbers. *J. Fluid Mech.*, 241: 1–22, 1992.

[2] J. Eggers and M. A. Fontelos. *Singularities: Formation, Structure, and Propagation.* Cambridge University Press, Cambridge, 2015.

[3] D. D. Joseph, J. Nelson, M. Renardy, and Y. Renardy. Two-dimensional cusped interfaces. *J. Fluid Mech.*, 223:383–409, 1991.

[4] É. Lorenceau, F. Restagno, and D. Quéré. Fracture of a viscous liquid. *Phys. Rev. Lett.*, 90:184501, 2003.

[5] J. Eggers. Air entrainment through free-surface cusps. *Phys. Rev. Lett.*, 86:4290–4293, 2001.

[6] E. Lorenceau, D. Quéré, and J. Eggers. Air entrainment by a viscous jet plunging into a bath. *Phys. Rev. Lett.*, 93:254501, 2004.

[7] E. Reyssat, E. Lorenceau, F. Restagno, and D. Quéré. Viscous jet drawing air into a bath. *Phys. Fluids*, 20:091107, 2008.

[8] J.-T. Jeong. Two-dimensional Stokes flow due to a pair of vortices below the free surface. *Phys. Fluids*, 22:082102, 2010.

[9] J.-T. Jeong. Formation of cusp on the free surface at low Reynolds number flow. *Phys. Fluids*, 11:521, 1999.

[10] J.-T. Jeong. Free surface deformation due to a source or sink in Stokes flow. *Eur. J. Mech. B/Fluids*, 26:720, 2007.

[11] L. K. Antanovskii. Formation of a pointed drop in taylor's four-roller mill. *J. Fluid Mech.*, 327:325, 1996.

[12] D. Crowdy. Exact solutions for two steady inviscid bubbles in the slow viscous flow generated by a four-roller mill. *J. Engin. Math.*, 44:311, 2002.

[13] G. I. Taylor. The formation of emulsions in definable fields of flow. *Proc. Roy. Soc. London A*, 146:501, 1934.

[14] S. Courrech du Pont and J. Eggers. Sink flow deforms the interface between a viscous liquid and air into a tip singularity. *Phys. Rev. Lett.*, 96:034501, 2006.

[15] S. Courrech du Pont and J. Eggers. Fluid interfaces with very sharp tips in viscous flow. *PNAS*, 117:32238, 2020.

[16] O. Hassager. Negative wake behind bubbles in non-Newtonian liquids. *Nature*, 279:402, 1979.

[17] J. Eggers and M. A. Fontelos. Cusps in interfacial problems. *Panoramas et Synthèses*, 38:69–90, 2012.

[18] J. Eggers and N. Suramlishvili. Singularity theory of plane curves and its applications. *Eur. J. Mech. B*, 65:107–131, 2017.

[19] L. D. Landau and E. M. Lifshitz. *Elasticity.* Pergamon: Oxford, 1984.

[20] S. Karpitschka, J. Eggers, A. Pandey, and J. H. Snoeijer. Cusp-shaped elastic creases and furrows. *Phys. Rev. Lett.*, 119: 198001, 2017.

[21] A. Chakrabarti, T. C. T. Michaels, S. Yin, E. Sun, and L. Mahadevan. The cusp of an apple. *Nature Phys.*, 17:1125, 2021.

[22] J. Nye. *Natural Focusing and Fine Structure of Light: Caustics and Wave Dislocations.* Institute of Physics Publishing, Bristol, 1999.

[23] J. Eggers, J. Hoppe, M. Hynek, and N. Suramlishvili. Singularities of relativistic membranes. *Geometric Flows*, 1:17–33, 2015.

[24] J. Eggers, T. Grava, M. A. Herrada, and G. Pitton. Spatial structure of shock formation. *J. Fluid Mech.*, 820:208–231, 2017.

[25] C. Kamal, J. Sprittles, J. H. Snoeijer, and J. Eggers. Dynamic drying transition via free-surface cusps. *J. Fluid Mech.*, 858:760, 2018.

[26] J. M. Rallison and A. Acrivos. A numerical study of the deformation and burst of a viscous drop in an extensional flow. *J. Fluid Mech.*, 89:191, 1978.
[27] J. Tanzosh, M. Manga, and H. A. Stone. Boundary integral methods for viscous free-boundary problems: Deformation of single and multiple fluid-fluid interfaces. In C. A. Brebbia and M. S. Ingber, editors, *Proceedings of Boundary Element Technologies VII*, page 19. Computational Mechanics, Southhampton, 1992.
[28] J. Eggers. Theory of bubble tips in strong viscous flows. *Phys. Rev. Fluids*, 6:044005, 2021.
[29] C. Pozrikidis. *Boundary Integral and singularity methods for linearized flow.* Cambridge University Press, Cambridge, 1992.
[30] E. J. Hinch. *Perturbation methods.* Cambridge University Press, Cambridge, 1991.
[31] J. P. K. Tillett. Axial and transverse stokes flow past slender axisymmetric bodies. *J. Fluid Mech.*, 44:401, 1970.
[32] M. Van Dyke. *Perturbation Methods in Fluid Mechanics.* The Parabolic Press, 1975.
[33] I. S. Gradshteyn and I. M. Ryzhik. *Table of Integrals Series and Products.* Academic: New York, 1980.
[34] W. H. Press, S. A. Teukolski, W. T. Vetterling, and B. P. Flannery. *Numerical Recipes.* Cambridge University Press, Cambridge, 1992.